

Reduction of the Pertechnetate Anion with Bidentate Phosphine Ligands

Evan Freiberg,^{†,‡} William M. Davis,[†] Terrence Nicholson,^{†,§} Alan Davison,^{*,†} and Alun G. Jones[§]*Department of Chemistry, Massachusetts Institute of Technology, Cambridge, Massachusetts 02139, and Department of Radiology, Harvard Medical School, Boston, Massachusetts 02115*

Received January 15, 2002

The reduction of ammonium pertechnetate with bis(diphenylphosphino)methane (dppm), and with diphenyl-2-pyridyl phosphine (Ph₂Ppy), has been investigated. The neutral Tc(II) complex, *trans*-TcCl₂(dppm)₂ (1), has been isolated from the reaction of (NH₄)[TcO₄] with excess dppm in refluxing EtOH/HCl. Chemical oxidation with ferricinium hexafluorophosphate results in formation of the cationic Tc(III) analogue, *trans*-[TcCl₂(dppm)₂](PF₆) (2). The dppm ligands adopt the chelating bonding mode in both complexes, resulting in strained four member metallocycles. With excess PhPpy, the reduction of (NH₄)[TcO₄] in refluxing EtOH/HCl yields a complex with one chelating Ph₂Ppy ligand and one unidentate Ph₂Ppy ligand, *mer*-TcCl₃(Ph₂Ppy-*P,N*)(Ph₂Ppy-*P*) (3). The cationic Tc(III) complexes, *trans*-[TcCl₂(Ph₂P(O)py-*N,O*)₂](PF₆) (4) and *trans*-[TcCl₂(dppmO-*P,O*)₂](PF₆) (5) (Ph₂P(O)py = diphenyl-2-pyridyl phosphine monoxide and dppmO = bis(diphenylphosphino)methane monoxide), have been isolated as byproducts from the reactions of (NH₄)[TcO₄] with the corresponding phosphine. The products have been characterized in the solid state and in solution *via* a combination of single-crystal X-ray crystallography and spectroscopic techniques. The solution state spectroscopic results are consistent with the retention of the bonding modes revealed in the crystal structures.

Introduction

The reduction of the pertechnetate anion with various phosphine ligands has been well studied over the past 25 years.^{1,2} This state of affairs is not surprising given the widespread use of phosphine ligands in transition metal chemistry and that pertechnetate is a widely used starting material in technetium chemistry. Deutsch and co-workers' thorough investigation into the reduction of pertechnetate with bidentate phosphine ligands, such as 1,2-bis(dimethylphosphino)ethane (dmpe), has led to the commercial development of Tc-99m radiopharmaceuticals.³

Two versatile bidentate phosphine ligands, the reactivities of which with the pertechnetate anion have not been studied, are bis(diphenylphosphino)methane (dppm) and diphenyl-2-pyridyl phosphine (Ph₂Ppy). Figure 1 shows structural formulas and various different bonding modes for the two

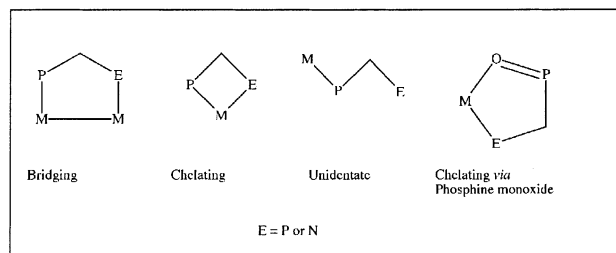
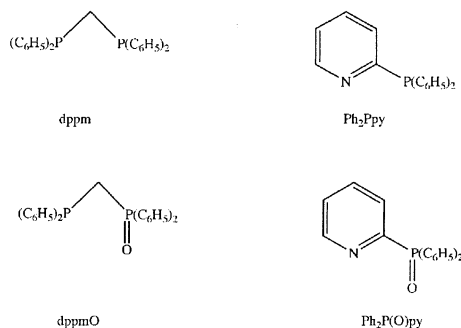


Figure 1. Structural formulas and selected bonding modes for bis(diphenylphosphino)methane, diphenyl-2-pyridyl phosphine, and their corresponding phosphine oxides.

ligands as well as their corresponding phosphine monoxides, bis(diphenylphosphino)methane monoxide (dppmO) and

* To whom correspondence should be addressed. E-mail: adavison@mit.edu. Fax: (617) 258-6989. Phone: (617) 253-1794.

[†] Massachusetts Institute of Technology.

[‡] Current address: Chemical Technology Division, Argonne National Laboratory, Argonne, IL 60439.

[§] Harvard Medical School.

(1) Mazzi, U.; DePaoli, G.; DiBernardo, P.; Magon, L. *J. Inorg. Nucl. Chem.* **1976**, *38*, 721–725.

(2) Baldas, J. *Adv. Inorg. Chem.* **1994**, *41*, 1–123.

(3) Deutsch, E. *Radiochim. Acta* **1993**, *63*, 195–197.

diphenyl-2-pyridyl phosphine monoxide (Ph₂P(O)py). As can be seen from Figure 1, dppm is capable of bridging two metal centers, resulting in a five member metallocycle, or chelating one metal center, resulting in a strained four member metallocycle. A metal–metal multiply bonded Tc₂(II,II) complex containing two bridging dppm ligands, Tc₂Cl₄(dppm)₂, has recently been prepared in our laboratory⁴ from a starting material already containing the Tc₂(II,II) core, namely Tc₂Cl₄(PEt₃)₄.⁵ For almost 20 years now, it has been known that the reduction of pertechnetate with 1,2-bis-(diphenylphosphino)ethane (dppe) results in monomeric complexes containing chelating dppe ligands;⁶ however, it remained unknown which bonding mode(s) dppm would adopt upon reaction with pertechnetate.

The bidentate phosphine ligand diphenyl-2-pyridyl phosphine is similar to dppm in that it contains a diphenyl phosphino moiety connected to another neutral, two electron donor *via* a one carbon backbone. This similarity manifests itself in similar bonding modes as shown in Figure 1. Although there have been recent reports of Tc–Ph₂Ppy complexes,^{7,8} the reactivity of Ph₂Ppy with pertechnetate has not been investigated. Interest in the reactivity of Ph₂Ppy with pertechnetate was further piqued by the report from our laboratory that the ligand reacts with perrhenate to form a Re–Ph₂P(O)py complex, ReOCl₃(Ph₂P(O)py-*N,O*).⁹ In addition, it has been observed that Ph₂Ppy reacts with (NBu₄)-[TcOCl₄], but the product(s) of that reaction were not identified.⁸ The reactions of ammonium pertechnetate with dppm and Ph₂Ppy are reported herein.

Experimental Section

General Considerations and Synthetic Procedures. Caution! Technetium-99 is a weak β⁻ emitter ($E = 0.292$ MeV, $t_{1/2} = 2.12 \times 10^5$ years). All work was carried out in laboratories approved for the use of low levels of radioactive materials. Precautions have been detailed elsewhere.¹⁰ All reagents were used as received except for the NBu₄PF₆ (TBAH) and ferrocene used in the electrochemical studies. The TBAH was recrystallized from acetone/ether, and the ferrocene was sublimed. All solvents were used as received. Degassed anhydrous solvents packaged under N₂ from Aldrich were used for work in the glovebox. Elemental analyses were carried out by Atlantic Microlab Inc., Norcross, GA 30071.

TcCl₂(dppm)₂ (1). To a 100 mL round-bottom flask were added 50 mL of EtOH and aqueous ammonium pertechnetate (2.0 mL, 0.60 mmol). To this stirred solution was added 2 mL of concentrated HCl followed immediately by dppm (2.8 g, 7.2 mmol), at which point the solution turned orange. After refluxing for 10 min, the

solution was red, and after 30 min, a yellow precipitate began to form. The reaction mixture was refluxed overnight and was filtered while still warm. The yellow powder was washed with ethanol and ether and dried *in vacuo*. Yield: 0.48 g (85% based on (NH₄)-[TcO₄]). FAB(+)-MS: m/z 937 [TcCl₂(dppm)₂]⁺, 902 [TcCl(dppm)₂]⁺, 553 [TcCl₂(dppm)]⁺, 518 [TcCl(dppm)]⁺. UV-vis (CH₂Cl₂): λ_{max} nm (ε M⁻¹ cm⁻¹) 232 (59.3 × 10⁴), 258 (38.6 × 10⁴), 410 (4.06 × 10³). IR (KBr): cm⁻¹ 3049.2 (w), 1482.1 (w), 1433.4 (s), 1091.3 (m), 741.0 (m), 730.7 (m), 693.9 (s), 504.2 (s). CV (200 mV/s, DMF, TBAH): $E_{1/2,ox} = -0.367$ V, $E_{1/2,red} = -1.72$ V. Yellow crystals of **1** were grown from acetone/pentane. Anal. Calcd for C₅₀H₄₄Cl₂P₄Tc: C, 63.98; H, 4.72; Cl, 7.55. Found: C, 63.59; H, 4.69; Cl, 7.94.

[TcCl₂(dppm)₂](PF₆) (2) Method 1. In a nitrogen filled glovebox, TcCl₂(dppm)₂ (0.27 g, 0.28 mmol), ferricinium hexafluorophosphate (0.13 g, 0.38 mmol), and 60 mL of THF were added to a 100 mL round-bottom flask. The reaction mixture was stirred for 25 min over which time most of the starting materials dissolved, and a clear red solution formed. The reaction mixture was gravity filtered. The filtrate was then concentrated to dryness, and the resulting red solid was washed with excess ether and filtered to remove ferrocene. The resulting crude powder was redissolved in 10 mL of acetone to which 50 mL of ether was carefully added. After standing overnight, a dark red crystalline solid was isolated, washed with ether, and dried *in vacuo*. Yield: 0.19 g (63% based on TcCl₂(dppm)₂). ¹H NMR (acetone-*d*₆): δ 18.5 (s, 45 Hz, 16 H, Ph *H*), 10.2 (s, 16 Hz, 8 H, Ph *H*), 8.06 (s, 16 Hz, 16 H, Ph *H*), -8.93 (s, 86 Hz, 4 H, methylene *H*). ESI(+)-MS: m/z 937 [TcCl₂(dppm)₂]⁺. UV-vis (CH₂Cl₂): λ_{max} nm (ε M⁻¹ cm⁻¹) 230 (43.3 × 10⁴), 276 (35.8 × 10⁴), 462 (954), 534 (979). IR (KBr): cm⁻¹ 3053.6 (w), 1483.4 (w), 1435.5 (s), 1097.1 (m), 837.1 (vs), 739.5 (m), 725.1 (m), 692.3 (s), 557.7 (m), 521.2 (w), 505.3 (s), 474.6 (w). CV (200 mV/s, DMF, TBAH): $E_{1/2,red} (1) = -0.368$ V, $E_{1/2,red} (2) = -1.72$ V. Red crystals of **2**·(CH₃)₂CO were grown from acetone/ether via the slow vapor diffusion technique. Anal. Calcd for C₅₀H₄₄Cl₂P₃F₆Tc: C, 55.42; H, 4.09; Cl, 6.54. Found: C, 55.11; H, 4.09; Cl, 6.71.

(2) Method 2. To a 250 mL round-bottom flask were added 50 mL of EtOH and aqueous ammonium pertechnetate (1.0 mL, 0.29 mmol). To this stirred solution, 2 mL of concentrated HCl was added, followed immediately by dppm (1.3 g, 3.4 mmol), at which point the solution turned orange. The reaction mixture was refluxed for 1 h. After cooling to room temperature, the reaction mixture was gravity filtered. An excess of NBu₄PF₆ (0.10 g, 0.61 mmol) was dissolved in 5 mL of EtOH and added to the clear red filtrate. The volume was reduced to ca. 15 mL at which point a red precipitate began to form. The red powder was washed with EtOH and ether and dried *in vacuo*. Yield: 0.055 g (18% based on (NH₄)-[TcO₄]).

TcCl₃(Ph₂Ppy-*P,N*)(Ph₂Ppy-*P*) (3). To a 250 mL round-bottom flask were added 50 mL of EtOH and aqueous ammonium pertechnetate (2.6 mL, 0.75 mmol). To this stirred solution was added 2 mL of concentrated HCl, followed immediately by Ph₂Ppy (2.7 g, 10 mmol). The reaction mixture immediately turned brown and was heated to reflux. After 10 min, the solution was red, and there was a goldenrod precipitate. The reaction was refluxed for 30 min and then allowed to cool to room temperature. Vacuum filtration yielded a goldenrod powder and a red filtrate. The goldenrod powder was washed with EtOH and ether and dried *in vacuo*. Yield: 0.40 g (64% based on (NH₄)[TcO₄]). ¹H NMR (dichloromethane-*d*₂): δ 18.4 (s, 30 Hz, 4 H, Ph *H*), 17.9 (s, 14 Hz, 1H, py *H*), 16.6 (s, 43 Hz, 4 H, Ph *H*), 15.0 (s, 14 Hz, 1 H, py *H*), 13.2 (s, 61 Hz, 1 H, py *H*), 10.7 (s, 14 Hz, 1 H, py *H*), 10.5 (s,

- (4) Freiberg, E.; Davison, A.; Jones, A. G.; Davis, W. M. *Inorg. Chem. Commun.* **1999**, 2, 516–518.
- (5) Burns, C. J.; Burrell, A. K.; Cotton, F. A.; Haefner, S. C.; Sattelberger, A. P. *Inorg. Chem.* **1994**, 33, 2257–2264.
- (6) Libson, K.; Barnett, B. L.; Deutsch, E. *Inorg. Chem.* **1983**, 22, 1695–1704.
- (7) Nicholson, T.; Hirsch-Kuchma, M.; Shellenbarger-Jones, A.; Davison, A.; Jones, A. G. *Inorg. Chim. Acta* **1998**, 267, 319–322.
- (8) Abram, U.; Alberto, R.; Dilworth, J. R.; Zheng, Y.; Ortner, K. *Polyhedron* **1999**, 18, 2995–3003.
- (9) Shellenbarger-Jones, A.; Nicholson, T.; Hirsch-Kuchma, M.; Davison, A.; Jones, A. G. *Technetium in Chemistry and Nuclear Medicine*; Nicolini, M., Mazzi, U., Eds.; Servizi Grafici Editoriali: Padova, Italy, 1998; Vol. 5, pp 183–186.
- (10) Davison, A.; Orvig, C.; Troop, H. S.; Sohn, M.; DePamphilis, B. V.; Jones, A. G. *Inorg. Chem.* **1980**, 19, 1988–1992.

Reduction of Pertechnetate Anion

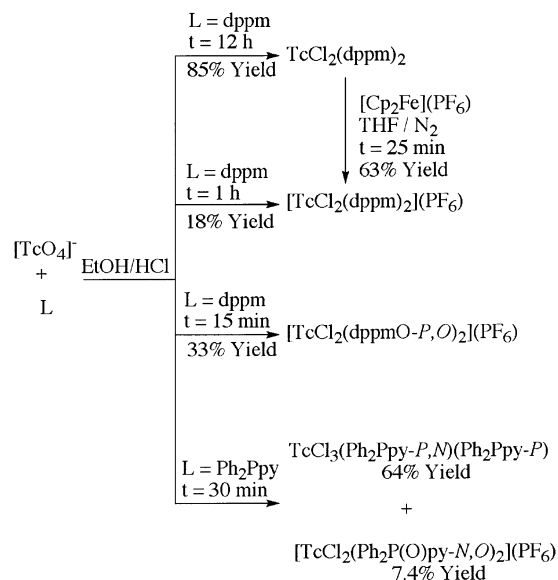
16 Hz, 4 H, Ph *H*), 9.67 (s, 16 Hz, 1 H, py *H*), 8.93 (s, 11 Hz, 1 H, py *H*), 8.39 (s, 15 Hz, 4 H, Ph *H*), 6.59 (s, 16 Hz, 4 H, Ph *H*), -17.8 (s, 106 Hz, 1 H, py *H*), -27.2 (s, 24 Hz, 1 H, py *H*). UV-vis (CH₂Cl₂): λ_{max} nm (ε M⁻¹ cm⁻¹) 232 (5.74 × 10³). IR (KBr): cm⁻¹ 3061.0 (w), 1570.1 (w), 1560.2 (w), 1481.1 (m), 1449.9 (m), 1433.7 (s), 1274.1 (w), 1186.0 (w), 1156.8 (w), 1089.4 (m), 1041.8 (w), 1021.8 (m), 772.1 (m), 754.1 (m), 743.2 (m), 694.3 (s), 520.8 (s), 502.0 (s). Goldenrod crystals of **3** were grown from dichloromethane/methanol/ether. Anal. Calcd for C₃₄H₂₈N₂Cl₃P₂Tc: C, 55.80; H, 3.86; N, 3.83; Cl, 14.53. Found: C, 55.31; H, 3.84; N, 3.78; Cl, 14.23.

[TcCl₂(Ph₂P(O)py-*N,O*)₂](PF₆) (4**).** The volume of the red filtrate described in the preceding paragraph was reduced, and an excess of NH₄PF₆ (0.25 g, 1.5 mmol) was dissolved in 10 mL of EtOH and added to the filtrate. After stirring for 2 h, a red-orange precipitate formed. The powder was washed with EtOH and ether and dried *in vacuo*. Yield: 0.056 g (7.4% based on (NH₄)[TcO₄]). ¹H NMR (acetone-*d*₆): δ 35.1 (s, 13 Hz, 2 H, py *H*), 29.4 (s, 14 Hz, 2 H, py *H*), 6.73 (t, 7 Hz, 8 H, Ph *H*), 6.60 (t, 4 Hz, 4 H, Ph *H*), 5.66 (s, 21 Hz, 8 H, Ph *H*), -23.9 (s, 17 Hz, 2 H, py *H*), -28.0 (s, 26 Hz, 2 H, py *H*). ESI(+)-MS: *m/z* 727 [TcCl₂(Ph₂P(O)py-*N,O*)₂]⁺. IR (KBr): cm⁻¹ 3074.4 (w), 1483.9 (w), 1458.4 (w), 1438.4 (m), 1121.8 (s), 1035.5 (m), 1014.6 (m), 996.3 (m), 838.4 (s), 777.4 (w), 750.2 (w), 734.5 (m), 726.5 (m), 689.9 (m), 650.1 (w), 616.4 (w), 572.2 (s), 557.8 (s), 534.5 (s), 455.7 (w). Orange crystals of **4** were grown from acetone/ether via the slow vapor diffusion technique.

[TcCl₂(dppmO-*P,O*)₂](PF₆) (5**).** To a 250 mL round-bottom flask were added 50 mL of EtOH and aqueous ammonium pertechnetate (1.0 mL, 0.29 mmol). To this stirred solution was added 2 mL of concentrated HCl immediately followed by dppm (1.3 g, 3.4 mmol) at which point the solution turned orange. The reaction mixture was gravity filtered after stirring for 15 min. The volume of the clear orange filtrate was reduced to ca. 25 mL. An excess of NH₄PF₆ (0.10 g, 0.61 mmol) was dissolved in 10 mL of EtOH and added to the filtrate. The volume of the filtrate was reduced until a red-orange precipitate formed. The red-orange powder was washed with ether and dried *in vacuo*. Yield: 0.11 g (33% based on (NH₄)[TcO₄]). ¹H NMR (acetone-*d*₆): δ 21.5 (s, 19 Hz, 8 H, Ph *H*), 9.78 (s, 15 Hz, 8 H, Ph *H*), 9.71 (t, 11 Hz, 4 H, Ph *H*), 7.30 (s, 16 Hz, 8 H, Ph *H*), 7.15 (t, 5 Hz, 4 H, Ph *H*), 5.90 (s, 19 Hz, 8 H, Ph *H*), -13.3 (s, 20 Hz, 4 H, methylene *H*). IR (KBr): cm⁻¹ 3055.2 (w), 1484.1 (w), 1437.4 (s), 1124.0 (s), 1098.7 (w), 1040.5 (w), 1024.3 (w), 997.8 (w), 840.1 (s), 777.5 (w), 740.0 (s), 690.9 (s), 557.6 (m), 506.6 (w), 472.2 (w). Orange crystals of **5** were grown from acetone/ether via the slow vapor diffusion technique.

Physical Measurements. The ¹H NMR spectra were recorded on a Varian 500 VXR spectrometer. The chemical shifts in the ¹H NMR spectra are referenced to the residual proton impurities in the deuterated solvents obtained from Cambridge Isotopes Laboratory. The electrospray ionization (+) spectra were recorded on a Bruker 3T FT-MS. The fast atom bombardment (+) spectrum of TcCl₂(dppm)₂ dissolved in *p*-nitrobenzyl alcohol matrix was recorded with a MAT 731 mass spectrometer equipped with an Ion Tech B11N FAB gun, operating at an accelerating voltage of 8 keV. The FAB gun produced a beam of 6–8 keV xenon neutrals. The UV-vis spectra were recorded on a Hewlett-Packard 8451A diode array spectrophotometer. The IR spectra were recorded on a Perkin-Elmer 1600 FTIR spectrometer. The cyclic voltammograms were recorded at room temperature in DMF using 0.1 M TBAH as supporting electrolyte and a CV-50W voltammetric analyzer (BAS). The electrochemical cell, purchased from Bioanalytical Systems,

Scheme 1



consisted of a stationary platinum disk working electrode and a platinum wire auxiliary electrode used in conjunction with a Ag wire pseudoreference electrode (Aldrich). The $E_{1/2}$ values, determined as $(E_{p,a} + E_{p,c})/2$, are reported relative to an internal ferrocene standard. The X-ray crystallographic data collection parameters and experimental details are given in the Supporting Information.

Results and Discussion

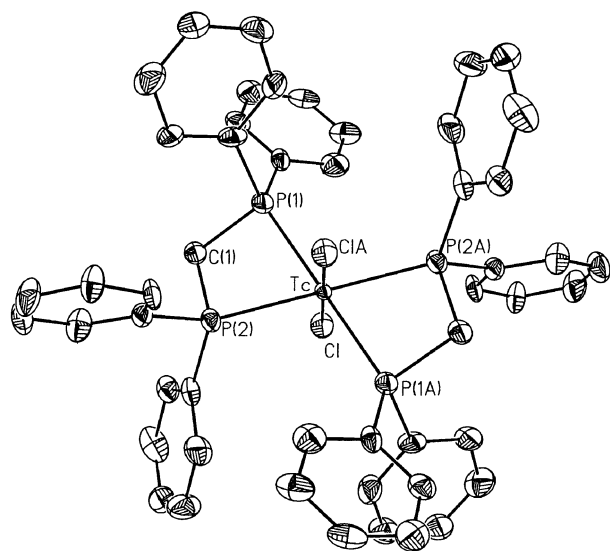
Synthesis and Characterization of **1 and **2**.** The reaction of aqueous ammonium pertechnetate with a 12 molar excess of dppm in refluxing EtOH/HCl results in the formation of **1** in 85% yield. The neutral Tc(II) complex precipitates out of the reaction mixture as a yellow powder. The reaction with dppm proceeds analogously to the reaction with dppe in that a neutral Tc(II) complex of the type TcCl₂(TDP)₂ (TDP = tertiary diphosphine ligand) precipitates out of refluxing EtOH/HCl. The syntheses of **1** and the other complexes presented herein are shown in Scheme 1.

Data collection parameters and crystal data for **1** are given in Table 1, and selected bond lengths and angles are listed in Table 2. As can be seen from the ORTEP in Figure 2, the two chlorine atoms occupy the axial positions, and the two dppm ligands occupy the equatorial plane about the technetium metal center which lies on an inversion center. The *trans* arrangement of the ligands is consistent with other structurally characterized [TcX₂(TDP)₂]^{0/+} (X = Cl, Br) complexes. The most noteworthy features of the crystal structure of **1** are the two four member metallocycles resulting from the chelating dppm ligands. The P–Tc–P bond angle, 69.05(9)°, is ca. 10° smaller than in TcCl₂-(dppe)₂¹¹ and is highly distorted from the ideal value of 90° for an octahedral complex. The methylene carbon atoms of the dppm ligands are distorted from ideal tetrahedral geometry with the P–C–P bond angle decreased to 96.5-(5)°. The P–Tc–P and P–C–P bond angles found in **1** are

(11) Libson, K.; Doyle, M. N.; Thomas, R. W.; Nelesnik, T.; Woods, M.; Sullivan, J. C.; Elder, R. C.; Deutsch, E. *Inorg. Chem.* **1988**, *27*, 3614–3619.

Table 1. Crystallographic Data for **1–5**

	1	2	3	4	5
empirical formula	C ₅₀ H ₄₄ Cl ₂ P ₄ Tc	C ₅₃ H ₅₀ Cl ₂ F ₆ OP ₅ Tc	C ₃₄ H ₂₈ Cl ₃ N ₂ P ₂ Tc	C ₃₄ H ₂₈ Cl ₂ F ₆ N ₂ O ₂ P ₃ Tc	C ₅₀ H ₄₄ Cl ₂ F ₆ O ₂ P ₅ Tc
fw	937.63	1140.68	730.87	872.39	1114.60
T, K	183(2)	183(2)	183(2)	183(2)	183(2)
wavelength, Å	0.71073	0.71073	0.71073	0.71073	0.71073
cryst syst	triclinic	triclinic	orthorhombic	monoclinic	monoclinic
space group	P1	P1	P ₂ ₁ ₂ ₁	C ₂ /c	C ₂ /c
a, Å	11.0256(11)	12.1601(13)	11.222(2)	28.813(17)	35.3200(11)
b, Å	11.2695(11)	12.9798(14)	15.089(3)	7.859(5)	11.5242(4)
c, Å	11.7812(12)	17.2293(18)	18.763(4)	15.229(6)	42.0610(12)
α, (deg)	92.771(2)	87.726(2)		94.28(3)	100.5630(10)
β, (deg)	104.474(2)	80.318(2)			
γ, (deg)	104.771(2)	72.725(2)			
V, Å ³	1360.7(2)	2559.6(5)	3176.9(12)	3439(3)	16830.2(9)
Z	1	2	4	4	12
ρ _{calcd} , g cm ⁻³	1.144	1.480	1.528	1.685	1.320
abs coeff, mm ⁻¹	0.508	0.602	0.834	0.783	0.549
cryst size, mm ³	0.15 × 0.1 × 0.1	0.22 × 0.25 × 0.38	0.05 × 0.2 × 0.2	0.05 × 0.1 × 0.3	0.15 × 0.3 × 0.3
reflns collected	4126	10476	13040	6745	27277
indept reflns	2535 (R _{int} = 0.0553)	7284 (R _{int} = 0.0350)	4570 (R _{int} = 0.0451)	2474 (R _{int} = 0.0471)	9045 (R _{int} = 0.0518)
refinement method	full-matrix least-squares on F ²	full-matrix least-squares on F ²	full-matrix least-squares on F ²	full-matrix least-squares on F ²	full-matrix least-squares on F ²
data/restraints/params	2533/0/260	7284/0/616	4570/0/379	2474/0/229	9043/0/900
GOF on F ²	1.182	1.099	1.264	1.274	1.175
final R indices	R1 = 0.0755, wR2 = 0.1767	R1 = 0.0376, wR2 = 0.0888	R1 = 0.0397, wR2 = 0.0792	R1 = 0.0539, wR2 = 0.1074	R1 = 0.0810, wR2 = 0.1858
[I > 2σ(I)]	wR2 = 0.1767	wR2 = 0.0888	wR2 = 0.0792	wR2 = 0.1074	wR2 = 0.1858
R indices (all data)	R1 = 0.0873, wR2 = 0.1901	R1 = 0.0435, wR2 = 0.0915	R1 = 0.0412, wR2 = 0.0797	R1 = 0.0655, wR2 = 0.1109	R1 = 0.0956, wR2 = 0.1960

**Figure 2.** ORTEP of TcCl₂(dppm)₂, **1**.**Table 2.** Selected Bond Lengths (Å) and Angles (deg) for **1**

Tc–Cl	2.432(3)	Tc–P(1)	2.402(3)
Tc–P(2)	2.441(3)		
P(1)–Tc–P(2)	69.05(9)	P(1)–Tc–P(2A)	110.95(9)
P(1)–C(1)–P(2)	96.5(5)	P(2)–Tc–P(1A)	110.95(9)
Tc–P(1)–C(1)	94.3(3)	Tc–P(2)–C(1)	93.9(3)
Cl–Tc–P(1)	85.64(9)	Cl–Tc–P(2)	81.25(9)

typical for complexes with chelating dppm ligands in the equatorial plane.¹² The Tc–Cl and Tc–P bond distances are unremarkable.

Solutions of **1** in chlorinated solvents, DMSO, DMF, and THF are not stable and turn orange-brown over the course of a day either under air or under an inert atmosphere. In

addition to its instability in solution, **1** is not very soluble. Solutions in DMF and DMSO cannot be concentrated above *ca.* 10 mM, whereas millimolar solutions could not be prepared in acetone, acetonitrile, or benzene. Attempts to definitively characterize **1** in solution *via* NMR spectroscopy failed in part because of the poor solubility properties of **1** and the paramagnetism expected for a d⁵ metal complex.

The FAB(+)-MS displays the parent ion, [TcCl₂(dppm)₂]⁺, and the fragments [TcCl(dppm)₂]⁺, [TcCl₂(dppm)]⁺, and [TcCl(dppm)]⁺, at *m/z* 937, 902, 553, and 518, respectively. The electronic absorption spectrum of **1** has two absorptions in the UV region, 232 nm (59.3 × 10⁴ M⁻¹ cm⁻¹) and 258 nm (38.6 × 10⁴ M⁻¹ cm⁻¹), and one in the visible region, 410 nm (4.06 × 10³ M⁻¹ cm⁻¹). Other than the observation of resonances consistent with the presence of dppm, the solid state IR spectrum is relatively uninformative.

Deutsch and co-workers have already shown that complexes of the type *trans*-[TcX₂(TDP)₂]^{0/+} have a rich redox chemistry associated with them.^{3,6} The cyclic voltammogram of **1** displays two reversible redox couples, the Tc(III/II) couple at –0.367 V and the Tc(II/I) couple at –1.72 V. The electrochemical data suggest that it should be possible to chemically oxidize the neutral Tc(II) complex to its analogous cationic Tc(III) complex using a relatively mild oxidizing agent.¹³ The reaction of **1** with [Cp₂Fe](PF₆) in THF at room temperature results in the formation of **2** in 63% yield. The cationic Tc(III) complex has also been isolated, in low yield, directly from ammonium pertechnetate and dppm in refluxing EtOH/HCl. The cyclic voltammogram of the chemically oxidized product, **2**, is very similar to that of **1**.

Data collection parameters and crystal data for **2**·(CH₃)₂CO are given in Table 1, selected bond lengths and

(12) Puddephatt, R. J. *Chem. Soc. Rev.* **1983**, 99–127.(13) Connelly, N. G.; Geiger, W. E. *Chem. Rev.* **1996**, 96, 877–910.

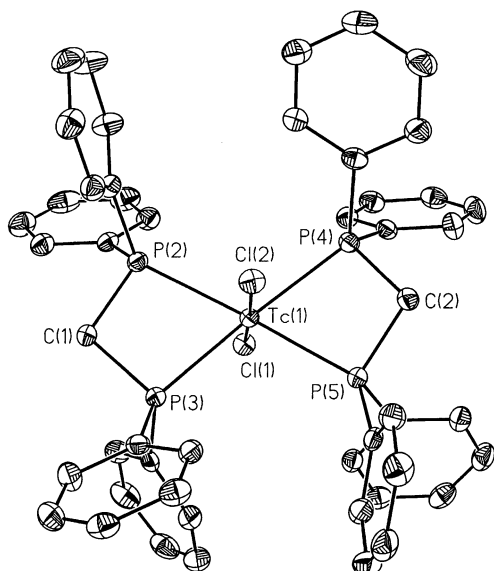


Figure 3. ORTEP of $[\text{TcCl}_2(\text{dppm})_2](\text{PF}_6)$, **2**, with the hexafluorophosphate counterion and the solvate omitted for clarity.

Table 3. Selected Bond Lengths (Å) and Angles (deg) for **2**

Tc(1)–Cl(1)	2.3006(8)	Tc(1)–Cl(2)	2.3332(9)
Tc(1)–P(2)	2.5109(9)	Tc(1)–P(3)	2.4583(8)
Tc(1)–P(4)	2.4987(9)	Tc(1)–P(5)	2.4616(9)
P(2)–Tc(1)–P(3)	69.37(3)	P(4)–Tc(1)–P(5)	68.06(3)
P(3)–C(1)–P(2)	99.70(15)	P(5)–C(2)–P(4)	97.67(15)
Tc(1)–P(2)–C(1)	94.33(10)	Tc(1)–P(3)–C(1)	96.35(10)
Tc(1)–P(4)–C(2)	92.78(11)	Tc(1)–P(5)–C(2)	93.94(10)
P(2)–Tc(1)–P(5)	174.98(3)	P(2)–Tc(1)–P(4)	115.02(3)
P(3)–Tc(1)–P(4)	171.60(3)	P(3)–Tc(1)–P(5)	107.05(3)
Cl(2)–Tc(1)–Cl(1)	176.67(3)		

angles are listed in Table 3, and an ORTEP is shown in Figure 3. As evidenced by the crystal structure, chemical oxidation of **1** does not significantly alter the arrangement of the P_4Cl_2 ligand set about the technetium metal center. Oxidation results in a decrease in the Tc–Cl bond distances and an increase in the Tc–P bond distances. Similar changes are also observed when comparing the bond lengths found in $\text{TcCl}_2(\text{dppe})_2$ and $[\text{TcCl}_2(\text{dppe})_2](\text{NO}_3)\cdot\text{HNO}_3$.^{6,11} The Tc–Cl and Tc–P bond lengths found in **2** are consistent with other structurally characterized Tc(III) compounds.¹⁴

In contrast to its neutral Tc(II) analogue, **2** is readily soluble in common organic solvents such as acetone, DMF, THF, and CH_2Cl_2 , and a well resolved ^1H NMR spectrum can be obtained. The assignment of the resonances is based upon the data listed in Table 4. The data show a dependence on the distance of the observed nuclei from the paramagnetic metal center. While this is consistent with a nuclear–electron dipolar interaction (pseudocontact), a contact interaction may also be contributing to the overall isotropic shifts.¹⁵ Other examples of six coordinate Tc(III) complexes which afford well resolved ^1H NMR spectra are $\text{TcCl}_3(\text{PMe}_2\text{Ph})_3$,¹ $\text{TcCl}_3(\text{py})_3$,¹⁶ $[\text{TcCl}_2(\text{PMe}_2\text{Ph})_2(\text{bpy})](\text{PF}_6)$,¹⁷ and $\text{Tc}(\text{F}_3\text{acac})_3$ ¹⁸ (py = pyridine, bpy = 2,2′-bipyridine, F_3acac = trifluoroacetyl-

Table 4. ^1H NMR Data for **2–5**^a

	2	5	4	3
methylene	–8.93, 86, 4 H	–13.3, 20, 4 H		
ortho	18.5, 45, 16 H	21.5, 19, 8 H		
meta	8.06, 16, 16 H	9.78, 15, 8 H		
para	10.2, 16, 8 H	9.71, 11, 4 H		
ortho′		5.90, 19, 8 H	5.66, 21, 8 H	
meta′		7.30, 16, 8 H	6.73, 7, 8 H	
para′		7.15, 5, 4 H	6.60, 4, 4 H	
py-a1			–28.0, 26, 2 H	–17.8, 106, 1 H
py-a2			35.1, 13, 2 H	15.0, 14, 1 H
py-a3			–23.9, 17, 2 H	–27.2, 24, 1 H
py-a4			29.4, 14, 2 H	17.9, 14, 1 H
py-b1				8.93, 11, 1 H
py-b2				10.7, 14, 1 H
py-b3				9.67, 16, 1 H
py-b4				13.2, 61, 1 H

^a The three values in each cell are the chemical shift (ppm), the linewidth at half height (Hz), and the integration. The (′) symbol denotes that those protons are on the phosphine oxide portion of the ligand. See Figure 5 for the pyridyl proton labeling scheme for **3** and **4**.

acetonato). Solutions in acetone are stable under nitrogen for at least one week but decompose slowly upon exposure to air, as evidenced by ^1H NMR spectroscopy.

The ESI(+)-MS consists of the parent ion peak, m/z 937, and it possesses the expected isotope splitting pattern. Significantly, in contrast to the fast atom bombardment mass spectrometry technique, which resulted in the fragments $[\text{TcCl}(\text{dppm})_2]^+$, $[\text{TcCl}_2(\text{dppm})]^+$, and $[\text{TcCl}(\text{dppm})]^+$ in the FAB(+)-MS of **1**, no fragmentation peaks are observed in the ESI(+)-MS of **2**. The electronic absorption spectrum of **2** has two absorptions in the UV region, 230 nm ($43.3 \times 10^4 \text{ M}^{-1} \text{ cm}^{-1}$) and 276 nm ($35.8 \times 10^4 \text{ M}^{-1} \text{ cm}^{-1}$), and two in the visible region, 462 nm ($954 \text{ M}^{-1} \text{ cm}^{-1}$) and 534 nm ($979 \text{ M}^{-1} \text{ cm}^{-1}$). The PF_6^- counterion is evidenced in the solid state IR spectrum with a very strong absorption at 837.1 cm^{-1} .

Synthesis and Characterization of 3. The reaction of aqueous ammonium pertechnetate with a 13 molar excess of Ph_2Ppy in refluxing EtOH/HCl results in the formation of **3** in 64% yield. The neutral Tc(III) complex precipitates directly from the reaction mixture as a goldenrod powder. As shown in the ORTEP in Figure 4, unlike the product of the reduction of pertechnetate with dppm, the two Ph_2Ppy ligands adopt two different bonding modes, chelating and unidentate. Data collection parameters and crystal data for **3** are given in Table 1, and selected bond lengths and angles are listed in Table 5. A consequence of the unidentate coordination of one Ph_2Ppy ligand via its phosphorus atom is an uncoordinated pyridyl nitrogen atom.

The three chlorine ligands are in a *mer* arrangement about the metal center, and the two phosphorus atoms are *cis* to one another. The arrangement of the ligand set in **3** is similar to that found by Nicholson *et al.* for $\text{TcCl}_2(\text{NO})(\text{Ph}_2\text{Ppy}-P,N)(\text{Ph}_2\text{Ppy}-P)$, **3-NO**, in which the chlorines and the nitrosyl occupy one meridian about the metal center.⁷ Complexes **3** and **3-NO** both have similar P–Tc–P and

(14) Tisato, F.; Refosco, F.; Bandoli, G. *Coord. Chem. Rev.* **1994**, *135/136*, 325–397.

(15) Holm, R. H. *Acc. Chem. Res.* **1969**, *2*, 307–316.

(16) Breikss, A. I.; Davison, A.; Jones, A. G. *Inorg. Chim. Acta* **1990**, *170*, 75–79.

(17) Breikss, A. I.; Nicholson, T.; Jones, A. G.; Davison, A. *Inorg. Chem.* **1990**, *29*, 640–645.

(18) Patterson, G. S.; Davison, A.; Jones, A. G.; Costello, C. E.; Maleknia, S. D. *Inorg. Chim. Acta* **1986**, *114*, 141–144.

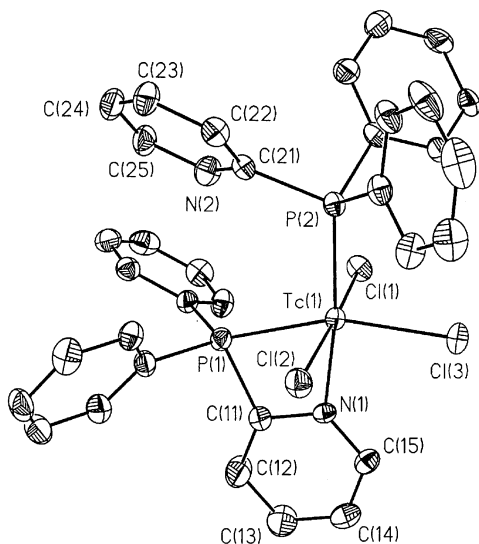


Figure 4. ORTEP of $\text{TcCl}_3(\text{Ph}_2\text{Ppy-P,N})(\text{Ph}_2\text{Ppy-P})$, **3**.

Table 5. Selected Bond Lengths (Å) and Angles (deg) for **3**

Tc(1)–N(1)	2.150(4)	Tc(1)–Cl(1)	2.3338(14)
Tc(1)–Cl(2)	2.3403(15)	Tc(1)–Cl(3)	2.4174(13)
Tc(1)–P(2)	2.4325(15)	Tc(1)–P(1)	2.4554(15)
N(1)–Tc(1)–Cl(1)	87.57(12)	N(1)–Tc(1)–Cl(2)	87.21(12)
Cl(1)–Tc(1)–Cl(2)	173.36(5)	N(1)–Tc(1)–Cl(3)	93.31(13)
Cl(1)–Tc(1)–Cl(3)	92.12(5)	Cl(2)–Tc(1)–Cl(3)	92.27(5)
N(1)–Tc(1)–P(2)	173.59(13)	Cl(1)–Tc(1)–P(2)	92.60(5)
Cl(2)–Tc(1)–P(2)	92.13(6)	Cl(3)–Tc(1)–P(2)	93.08(5)
N(1)–Tc(1)–P(1)	66.36(12)	Cl(1)–Tc(1)–P(1)	88.00(5)
Cl(2)–Tc(1)–P(1)	86.16(5)	Cl(3)–Tc(1)–P(1)	159.66(5)
P(2)–Tc(1)–P(1)	107.24(5)	C(11)–P(1)–Tc(1)	82.44(18)
P(1)–C(11)–N(1)	103.3(4)	C(11)–N(1)–Tc(1)	107.8(3)

P–Tc–N bond angles, $107.24(5)^\circ$ and $66.36(12)^\circ$ found in **3**, and $107.82(5)^\circ$ and $66.09(13)^\circ$ found in **3-NO**. A comparison of the three Tc–Cl bond lengths found in **3**, 2.3338(14), 2.3403(15), and 2.4174(13) Å, for Tc(1)–Cl(1), Tc(1)–Cl(2), and Tc(1)–Cl(3), respectively, shows the *trans* effect that P(1) has on the Tc(1)–Cl(3) bond. The Tc(1)–Cl(1) and Tc(1)–Cl(2) bond distances, as well as the two Tc–P and the Tc(1)–N(1) bond distances, are unremarkable.

The ^1H NMR spectrum of **3** consists of two sets of Ph_2Ppy resonances, one for the chelating ligand and one for the unidentate ligand. This result is in contrast to the ^1H NMR spectra of **2** (*vide supra*), **4**, and **5** (*vide infra*), in which there is only one set of dppm , $\text{Ph}_2\text{P}(\text{O})\text{py}$, and dppmO resonances, respectively. The lowering of the symmetry in **3**, relative to **2**, **4**, and **5**, manifests itself in the increased number of resonances observed in the ^1H NMR spectrum. Using a 2D ^1H gCOSY spectrum of the complex, the eight resonances due to the pyridyl protons can be divided into two sets of four, corresponding to the coordinated and the uncoordinated pyridyl rings. The determination of which set of resonances was due to the coordinated pyridyl ring, labeled ring a in Figure 5, was based upon comparisons with $\text{TcCl}_3(\text{py})_3$,¹⁶ and **4**, which only contain coordinated pyridyl rings. The assumption was made that the resonances due to the protons at the positions labeled a1 and b4 would be the broadest for the coordinated and uncoordinated pyridyl rings, respectively.

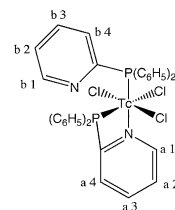


Figure 5. Pyridyl proton labeling scheme for **3**. An analogous scheme is used for the coordinated pyridyl rings found in **4**.

The other positions are assigned on the basis of the cross-peaks observed in the 2D ^1H gCOSY experiment.

From Table 4, it can be seen that the protons on the coordinated pyridyl ring experience larger isotropic shifts than the protons on the uncoordinated pyridyl ring. The coordinated pyridyl ring is closer to the paramagnetic metal center than the uncoordinated pyridyl ring, and therefore, the protons on the coordinated pyridyl ring may experience a stronger pseudocontact interaction.¹⁵ Furthermore, the protons on the coordinated pyridyl ring may experience a contact interaction with the metal center *via* the π -system of the pyridyl ring,^{15,16} which can interact with metal based orbitals having the proper energy and symmetry. In contrast, the π -system of the uncoordinated pyridyl ring cannot interact directly with metal based orbitals.

The IR and electronic absorption spectra of **3** are relatively uninformative. The UV transition, 232 nm ($5.74 \times 10^3 \text{ M}^{-1} \text{ cm}^{-1}$), has a shoulder which tails into the visible region of the spectrum and therefore contributes to the color of the complex.

Synthesis and Characterization of 4 and 5. The reaction of aqueous ammonium pertechnetate with a 12–13 molar excess of dppm or Ph_2Ppy in refluxing EtOH/HCl results in the formation of (in addition to **1–3**) Tc(III) byproducts with the general formula $[\text{TcCl}_2(\text{phosphine oxide-}E,O)_2]^+$ ($E = \text{P}$ or N). The bis- $\text{Ph}_2\text{P}(\text{O})\text{py}$ complex, **4**, was isolated, in 7% yield, from the filtrate when **3** was removed from the reaction mixture. The bis- dppmO complex, **5**, was originally isolated from the filtrate when **1** was removed from the reaction mixture. Subsequently, the reaction of pertechnetate with a 12 molar excess of dppm was performed at room temperature to increase the yield of **5**. The solid state IR spectra of **4** and **5** display characteristic P=O stretching frequencies at 1121.8 and 1124.0 cm^{-1} , respectively. The PF_6^- counterions are evidenced by strong absorptions at 838.4 and 840.1 cm^{-1} in the IR spectra of **4** and **5**, respectively. The ESI(+)-MS of **4** shows no fragmentation of the parent ion, $[\text{TcCl}_2(\text{Ph}_2\text{P}(\text{O})\text{py-N,O})]^+$, which corresponds to the peak at m/z 727.

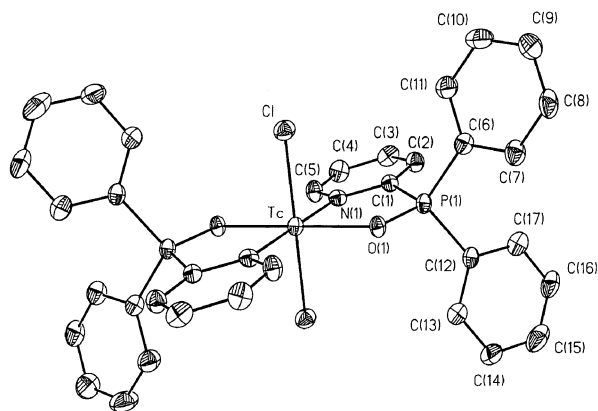
Although the ability of tertiary phosphines to act as oxygen atom acceptors is well established,¹⁹ it cannot be stated with any degree of certainty that the phosphine oxide complexes isolated under the reaction conditions employed herein are the result of oxygen atom transfer from the metal. Another scenario is that the tertiary phosphines are oxidized to their corresponding phosphine monoxides (i.e., dppmO and $\text{Ph}_2\text{P}(\text{O})\text{py}$) in refluxing EtOH/HCl , and then they coordinate to the technetium metal center. The phosphine oxide dppmO

(19) Holm, R. H. *Chem. Rev.* **1987**, *87*, 1401–1449.

Table 6. Selected Bond Lengths (Å) and Angles (deg) for **4**

Tc–Cl	2.3514(17)	Tc–O(1)	2.107(3)
Tc–N(1)	2.122(4)	O(1)–P(1)	1.520(4)
O(1)–Tc–N(1)	82.58(14)	O(1)–Tc–N(1)#1 ^a	97.42(14)
O(1)–Tc–Cl	88.80(10)	O(1)–Tc–Cl#1	91.20(10)
N(1)–Tc–Cl	89.36(12)	N(1)–Tc–Cl#1	90.64(12)
Tc–O(1)–P(1)	118.09(18)	Tc–N(1)–C(1)	123.3(4)
O(1)–P(1)–C(1)	106.2(2)	N(1)–C(1)–P(1)	113.3(4)

^a Symmetry transformations used to generate equivalent atoms: #1 $-x + 1/2, -y + 1/2, -z + 1$.

**Figure 6.** ORTEP of $[\text{TcCl}_2(\text{Ph}_2\text{P}(\text{O})\text{py-}N,\text{O})_2](\text{PF}_6)_4$, **4**, with the hexafluorophosphate counterion omitted for clarity.

has been shown to coordinate to Re(V)–oxo starting materials to yield Re(V)–oxo complexes containing chelating dppmO ligands such as $\text{Re}^{\text{V}}\text{OCl}_3(\text{dppmO-}P,\text{O})$.²⁰ The isolation of phosphine oxide complexes *via* the reduction of pertechnetate with excess phosphine in refluxing EtOH/HCl has not been previously reported.

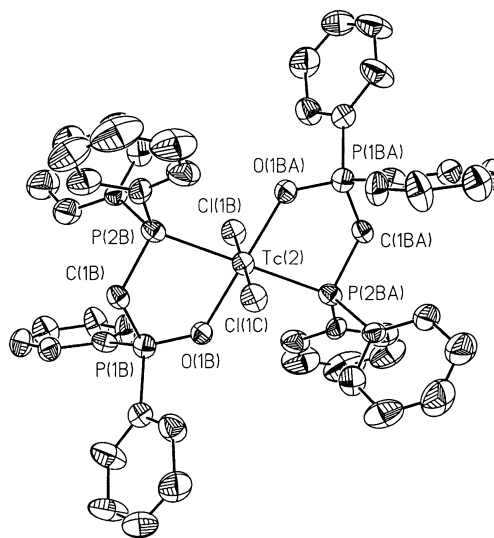
Data collection parameters and crystal data for **4** are given in Table 1, selected bond lengths and angles are listed in Table 6, and an ORTEP is shown in Figure 6. The structure of **4** is similar to that of **1** and **2** in that the two chlorine atoms occupy the axial positions and the two chelating ligands, in this case $\text{Ph}_2\text{P}(\text{O})\text{py}$, occupy the equatorial plane about the technetium metal center, which lies on an inversion center. The five member metallocycles resulting from the chelating $\text{Ph}_2\text{P}(\text{O})\text{py}$ ligands are much less strained than the four member metallocycles found in **1** and **2**, as evidenced by the larger bite angle found in **4**, $82.58(14)^\circ$. This value is similar to the bite angle found in $\text{ReCl}_3(\text{Ph}_2\text{P}(\text{O})\text{py-}N,\text{O})\text{-}(\text{PPh}_3)$, $81.8(2)^\circ$.⁹ Again, the observed Tc–Cl and the Tc–N bond distances are unremarkable. The structural parameters associated with the phosphine oxide portion of the complex are included in the discussion of the structure of **5**.

The ^1H NMR spectrum of **4** is consistent with the solid state structure. The four resonances due to the pyridyl protons were assigned on the basis of the data listed in Table 4. A 2D ^1H gCOSY spectrum confirmed that the four resonances belong to the same ring system. With the assumption that the proton at position a1 would have the broadest resonance, the assignments were made utilizing the 1D and 2D NMR data. The other three resonances in the spectrum are assigned to the meta', para', and ortho' phenyl protons using the data

Table 7. Selected Bond Lengths (Å) and Angles (deg) for **5**

Tc(2)–O(1B)	2.109(6)	Tc(2)–Cl(1B)	2.329(2)
Tc(2)–P(2B)	2.449(3)	P(1B)–O(1B)	1.503(7)
P(2B)–Tc(2)–O(1B)	84.5(2)	P(2B)–Tc(2)–O(1BA) ^a	95.5(2)
Tc(2)–O(1B)–P(1B)	123.8(4)	Tc(2)–P(2B)–C(1B)	100.3(3)
P(2B)–C(1B)–P(1B)	109.2(5)	C(1B)–P(1B)–O(1B)	110.3(4)
O(1B)–Tc(2)–Cl(1B)	89.7(2)	O(1B)–Tc(2)–Cl(1C)	90.3(2)
P(2B)–Tc(2)–Cl(1B)	93.95(9)	P(2B)–Tc(2)–Cl(1C)	86.05(9)

^a Symmetry transformations used to generate equivalent atoms [O(1BA) and Cl(1C)]: #1 $-x + 1, -y, -z$.

**Figure 7.** ORTEP of $[\text{TcCl}_2(\text{dppmO-}P,\text{O})_2](\text{PF}_6)_4$, **5**, with cation A and the hexafluorophosphate counterion omitted for clarity.

listed in Table 4. The (') symbol is to denote that these phenyl protons are on the phosphine oxide portion of the ligand. The pyridyl protons in **4** experience a much greater isotropic shift¹⁵ than the phenyl protons. This is not surprising given that the π -system of the pyridyl ring can interact directly with metal based orbitals having the proper energy and symmetry, and that the pyridyl ring is closer to the paramagnetic metal center.

Data collection parameters and crystal data for **5** are given in Table 1, selected bond lengths and angles are given in Table 7, and an ORTEP is shown in Figure 7. There are two $[\text{TcCl}_2(\text{dppmO-}P,\text{O})_2]^+$ cations in the asymmetric unit, as well as two PF_6^- counterions. Cation A, which contains Tc(1), and cation B, which contains Tc(2), are both very similar, and only the structural parameters found in cation B will be discussed. The Tc atom in cation B lies on an inversion center. The structure of **5** is similar to that of **4** in that the two phosphine oxide oxygen atoms are *trans* to one another. As evidenced by the P–Tc–O and P–C–P bond angles found in **5**, $84.5(2)^\circ$ and $109.2(5)^\circ$, respectively, the five member metallocycles resulting from the chelating dppmO ligands are less strained than the four member metallocycles found in **1** and **2**. The Tc–Cl and Tc–P bond distances are again unremarkable.

The Tc–O and O=P bond lengths found in **5** are 2.109(6) and 1.503(7) Å. These values are similar to those found in **4**, 2.107(3) and 1.520(4) Å, and are consistent with other

(20) Katti, K. V.; Barnes, C. L. *Inorg. Chem.* **1992**, *31*, 4231–4235.

structurally characterized phosphine oxide complexes.^{9,20–26} The M–O=P bond angle found in **4**, 118.09(18)°, is similar to that found in ReCl₃(Ph₂P(O)py-*N,O*)(PPh₃), 115.5(3)°.⁹ The M–O=P bond angles found in ReOCl₃(dppmO-*P,O*)²⁰ and ReCl₄(dppmO-*P,O*),²² ca. 130°, are somewhat larger than in **5**, 123.8(4)°. However, the M–O=P bond angle in various complexes containing chelating dppmO ligands appears to be quite variable as evidenced by the small M–O=P bond angle found in PdCl₂(dppmO-*P,O*), 108.1(2)°.²³

The ¹H NMR spectrum of **5** consists of a set of resonances due to the phenyl protons on the phosphine portion of the ligand and a set due to the phenyl protons on the phosphine oxide portion (denoted with the (′) symbol). In addition, there is a resonance due to the methylene protons on the dppm backbone. The assignments are based upon the data listed in Table 4. Comparisons to **2** and **4** were useful because **2** contains phenyl but no phenyl′ protons, whereas **4** contains phenyl′ but no phenyl protons. A 2D ¹H gCOSY spectrum of **5** confirms that the resonances assigned to ortho, meta, and para belong to the same ring system, and that the resonances assigned to ortho′, meta′, and para′ belong to a separate ring system. In addition, as expected, no cross-peak is observed for the resonance assigned to the methylene protons.

Conclusion

The reduction reactions of ammonium pertechnetate with the versatile bidentate phosphine ligands bis(diphenylphos-

phino)methane and diphenyl-2-pyridyl phosphine have been investigated. The reduction of ammonium pertechnetate with excess dppm results in a monomeric complex in the +2 oxidation state containing chelating dppm ligands. The Tc(III) compound can be prepared in good yield *via* chemical oxidation of this Tc(II) species. With Ph₂Ppy, the reduction of ammonium pertechnetate results in a monomeric complex in the +3 oxidation state with one chelating Ph₂Ppy ligand and one unidentate Ph₂Ppy ligand. Phosphine oxide containing complexes with the general formula [TcCl₂(phosphine oxide-*E,O*)₂](PF₆) (E = P or N) have been isolated as byproducts in the reduction of ammonium pertechnetate with excess dppm or Ph₂Ppy. The complexes have been characterized both in the solid state, primarily *via* single crystal X-ray crystallography, and in solution, primarily *via* ¹H NMR spectroscopy. The effects that the different bonding modes of dppm and Ph₂Ppy, (i.e., chelating, chelating *via* the corresponding monoxide, unidentate) have on the structural parameters and the ¹H NMR spectra of the complexes were discussed.

Acknowledgment. The authors thank L. Li and Dr. J. Simpson of the MIT Department of Chemistry Instrumentation Facility (DCIF) and D. Kramer for assistance obtaining the mass spectra and the 2D ¹H gCOSY spectra. Professor Cummins and Yi-Chou Tsai are acknowledged for the use of and the assistance with the CV-50W voltammetric analyzer. Financial support to E.F., T.N., A.D., and A.G.J. (NIH) and to the DCIF (DBI-9729592) is acknowledged.

Supporting Information Available: X-ray crystallographic files in CIF format for **1–5**, X-ray crystallographic data collection parameters and experimental details for **1–5**, ¹H NMR spectra for **2–5**, 2D ¹H gCOSY spectra for **3–5**, mass spectra for **1**, **2**, and **4**, and a cyclic voltammogram for **1**. This material is available free of charge via the Internet at <http://pubs.acs.org>.

IC020032I

- (21) Kaden, L.; Lorenz, B.; Kirmse, R.; Stach, J.; Behm, H.; Beurskens, P. T.; Abram, U. *Inorg. Chim. Acta* **1990**, *169*, 43–48.
- (22) Rossi, R.; Marchi, A.; Marvelli, L.; Magon, L.; Peruzzini, M.; Casellato, U.; Graziani, R. *Inorg. Chim. Acta* **1993**, *204*, 63–71.
- (23) Brassat, I.; Englert, U.; Keim, W.; Keitel, D. P.; Killat, S.; Suranna, G.; Wang, R. *Inorg. Chim. Acta* **1998**, *280*, 150–162.
- (24) Menon, M.; Pramanik, A.; Bag, N.; Chakravorty, A. *Inorg. Chem.* **1994**, *33*, 403–404.
- (25) Larsen, S. K.; Pierpont, C. G.; DeMunno, G.; Dolcetti, G. *Inorg. Chem.* **1986**, *25*, 4828–4831.
- (26) Baird, D. M.; Fanwick, P. E.; Barwick, T. *Inorg. Chem.* **1985**, *24*, 3753–3758.